

## High-spin states and band structure in $^{76}\text{Br}$

J. C. Wells

*Physics Department, Tennessee Technological University, Cookeville, Tennessee 38501  
and Physics Division, Oak Ridge National Laboratory, Oak Ridge, Tennessee 37830*

R. L. Robinson, H. J. Kim, and R. O. Sayer

*Physics Division, Oak Ridge National Laboratory, Oak Ridge, Tennessee 37830*

R. B. Piercey, A. V. Ramayya, J. H. Hamilton, and C. F. Maguire

*Physics Department, Vanderbilt University, Nashville, Tennessee 37235*

K. Kumar, R. W. Eastes,\* and M. E. Barclay†

*Physics Department, Tennessee Technological University, Cookeville, Tennessee 38501*

A. J. Caffrey

*Physics Department, The Johns Hopkins University, Baltimore, Maryland 21218*

(Received 17 February 1981)

High-spin states of  $^{76}\text{Br}$  have been investigated through observations of  $\gamma$  rays produced in the  $^{66}\text{Zn}(^{12}\text{C},pn)$  reaction by bombarding an enriched  $^{66}\text{Zn}$  target with 38.0-MeV  $^{12}\text{C}$  ions. Measurements were made of  $\gamma$ -ray singles and  $\gamma$ - $\gamma$  coincidence spectra,  $\gamma$ -ray angular distributions, and  $\gamma$ -ray linear polarizations. Level energies, decay modes, spins and parities,  $\gamma$ -ray branching ratios, and  $\gamma$ -ray radiative admixtures were deduced. There is evidence for a strongly excited  $\Delta J = 1$  quasirotational band.

[NUCLEAR REACTIONS  $^{66}\text{Zn}(^{12}\text{C},pn)$   $E = 38$  MeV; measured  $E_\gamma$ ,  $I_\gamma$ ,  $\gamma(\theta)$ ,  $\gamma$ -ray linear polarizations;  $^{76}\text{Br}$  deduced levels,  $J$ ,  $\pi$ ,  $\delta$ ,  $\gamma$  branching.]

### I. INTRODUCTION

As part of a systematic study of high-spin states and band structure of nuclei in the mass range around  $A = 70$ , we have investigated high-spin states of  $^{76}\text{Br}$ , produced by the  $^{66}\text{Zn}(^{12}\text{C},pn\gamma)$  reaction. We have made measurements of  $\gamma$ -ray singles and  $\gamma$ - $\gamma$  coincidence spectra, angular distributions, and linear polarizations. We have also constructed an energy level scheme, and have deduced spins and parities,  $\gamma$ -ray branching ratios, and radiative admixtures for some of the levels.

Many low-spin states of  $^{76}\text{Br}$  have been reported by Paradellis *et al.*<sup>1</sup> and by Lode *et al.*<sup>2</sup> from the decay of  $^{76}\text{Kr}$ , and by Lueders *et al.*<sup>3</sup> with the  $^{76}\text{Se}(p,n\gamma)$  reaction. Behar *et al.*,<sup>4</sup> using the  $^{75}\text{As}(\alpha,3n\gamma)$  reaction, have reported eight  $\gamma$  rays assigned to a quasirotational band which begins on a  $6^-$  state at 1016 keV and terminates on the  $1^-$  ground state. Of these  $\gamma$  rays, only the 142-keV transition was observed in Refs. 1–3, and none of these incorporated it into a level scheme. This led Lueders *et al.*<sup>3</sup> to comment that the band was very possibly built on a long-lived isomeric level rather than on the ground state.

Subsequently, Schmidt-Ott *et al.*<sup>5</sup> and Kreiner *et al.*<sup>6</sup> reported a long-lived ( $\approx 1.4$ -s) isomeric state in  $^{76}\text{Br}$ . Both assigned the state a spin and

parity of  $J^\pi = 4^+$ , and the latter suggested that this state may be the bandhead for the quasirotational band. Mariscotti *et al.*<sup>7</sup> have reported a similar situation in  $^{78}\text{Rb}$ , as have Behar *et al.*<sup>8</sup> in  $^{82}\text{Rb}$ .

We have observed all of the  $\gamma$  rays reported by Behar *et al.*<sup>4</sup> plus a number of others. Our results agree with theirs.

### II. EXPERIMENTAL PROCEDURE

A target of 20-mg/cm<sup>2</sup> enriched  $^{66}\text{Zn}$  on a thick Ni backing was bombarded with 38.0-MeV  $^{12}\text{C}$  ions from the ORNL EN tandem accelerator. Excited states of  $^{76}\text{Br}$  were populated by the  $^{66}\text{Zn}(^{12}\text{C},pn)$  reaction.

Coincidence measurements were made with two large-volume Ge(Li) detectors placed at  $0^\circ$  and  $90^\circ$  with respect to the beam direction, and 5 cm from the target. The angular distributions of the  $\gamma$  rays were measured at  $0^\circ$ ,  $55^\circ$ , and  $90^\circ$ , with respect to the beam direction using a large-volume Ge(Li) detector placed 12 cm from the target. A second Ge(Li) detector at  $135^\circ$  served as a monitor, and was used to normalize the  $\gamma$ -ray intensities at each of the three angles. A  $^{226}\text{Ra}$  source was placed at the target position at the conclusion of the angular distribution experiments to determine the magnitude of the cor-

rection for the target's not being at the exact center of rotation of the angular correlation table. This source was also used to determine the energy and efficiency calibrations of the detectors.

Linear polarizations of the  $\gamma$  rays were measured with a  $\gamma$ -ray polarimeter placed 16 cm from the target at an angle of  $90^\circ$  to the beam direction. The polarimeter, developed at The Johns Hopkins University, has been described in Ref. 9. Our experimental details were identical with those described in Ref. 10.

### III. ANALYSIS AND RESULTS

#### A. Level scheme

A representative singles  $\gamma$ -ray spectrum and a  $\gamma$ - $\gamma$  coincidence-gated spectrum are shown in Figs. 1 and 2. The results of  $\gamma$ - $\gamma$  coincidence measurements were used to identify those  $\gamma$  rays belonging to  $^{76}\text{Br}$  and to construct a level scheme, which is shown in Fig. 3. The  $\gamma$ -ray energies are given in Table I and in Fig. 3. Relative  $\gamma$ -ray intensities obtained from the singles spectra were used to establish the order of the cascades. These intensities are given in Table I, and are indicated graphically by the widths of the transition arrows in the level scheme in Fig. 3. The level energies were obtained by a least-squares fit to all of the  $\gamma$ -ray energies. A summary of our coincidence data is presented in Table II.

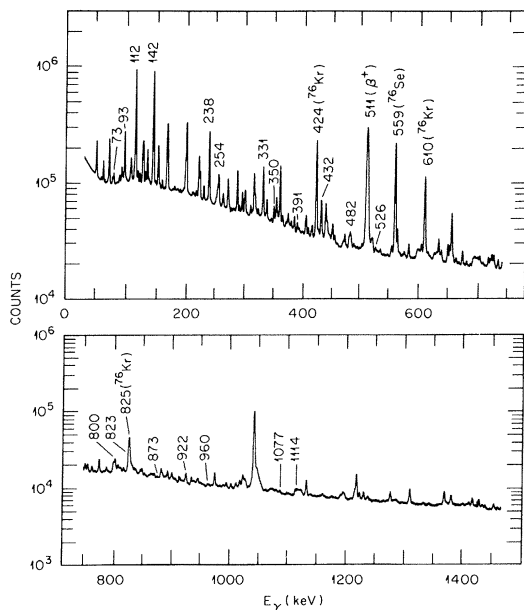


FIG. 1. In-beam singles  $\gamma$ -ray spectrum resulting from the bombardment of a  $^{66}\text{Zn}$  target with 38.0-MeV  $^{12}\text{C}$  ions. Energies are in keV. Unless otherwise indicated, those photopeaks which are labeled are assigned to  $^{76}\text{Br}$ .

Identification of  $\gamma$  rays belonging to  $^{76}\text{Br}$  was based on coincidences with both the 142- and 112-keV  $\gamma$  rays; these having been established as belonging to  $^{76}\text{Br}$  by Behar *et al.*<sup>4</sup> With the exception of the 800- and 1114-keV  $\gamma$  rays, the placements of all of the  $\gamma$  rays in the level scheme are well established by the coincidence relationships. The 800-keV  $\gamma$  ray is seen weakly in the 331-keV gate, but neither the 331- nor the 93-keV  $\gamma$  ray is seen in the 800-keV gate, raising the possibility that the 800-keV  $\gamma$  ray should terminate at the 492-keV level. A weak coincidence is seen between the 1114- and the 482-keV  $\gamma$  rays in both the 482- and 1114-keV gates, and although the indicated placement of the 1114-keV  $\gamma$  ray seems probable, the possibility of its terminating at the 1409-keV level is not completely ruled out. Placement of the 73-keV  $\gamma$  ray appears valid except for a problem of its coincidence with itself and with the 1077-keV  $\gamma$  ray.

The 800-, 823-, and 922-keV  $\gamma$  rays showed definite coincidences with  $\gamma$  rays from  $^{76}\text{Kr}$ , and the 800-keV  $\gamma$  ray with  $^{76}\text{Se}$ , also. In addition, to these doublets, the 73-, 254-, and 482-keV  $\gamma$  rays were so close to impurity peaks in the singles spectra that resolution was difficult.

It is seen in Table II that there are  $\gamma$  rays with energies of 124, 166, 199, 220, 222, 300, 338, 355, and 1039 keV that are in coincidence with two or more  $\gamma$  rays assigned to  $^{76}\text{Br}$ . Some of these may well originate in  $^{76}\text{Br}$ , also, but it was not possible to incorporate any of them into the level scheme in a consistent way.

#### B. Angular distributions

The angular distribution coefficients  $A_2 = a_2/a_0$  and  $A_4 = a_4/a_0$  were extracted from the expression

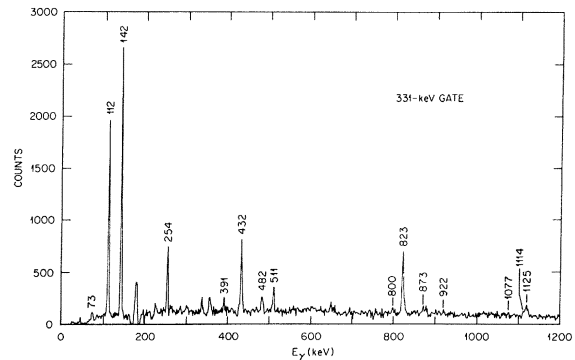


FIG. 2. Selected  $\gamma$ - $\gamma$  coincidence-gated spectrum of transitions in  $^{76}\text{Br}$ . Energies are in keV. The spectrum shown is the result of the difference between two spectra, one with a gate set on the 331-keV photopeak, and the other with a gate set on the continuum above and below the photopeak.

TABLE I. Energies, relative intensities, angular distributions, and linear polarizations of  $\gamma$  rays in  $^{76}\text{Br}$ . The numbers in parentheses give the probable error in the last significant figures.

$E_\gamma$ (keV)	$L_\gamma$	$A_{2\text{exp}}$	$A_{4\text{exp}}$	$P_{\text{exp}}$	$P_{\text{cal}}^b$
72.9 (2)	27 (4)				
93.4 (2)	257 (13)	-0.23 (4)	-0.09 (4)		
112.0 (2)	786 (40)	-0.33 (4)	-0.04 (4)	0.51 (18)	
142.2 (2)	1000 (50)	-0.39 (3)	-0.02 (3)	0.28 (14)	
237.9 (2)	361 (17)	-0.40 (3)	-0.03 (3)	-0.12 (3)	
253.9 (5)	134 (7)	0.17 (6)	-0.06 (6)	0.14 (6)	0.24 (12)
331.3 (2)	254 (13)	0.33 (3)	-0.05 (3)	0.43 (6)	0.56 (7)
350.1 (2)	40 (10)	-0.20 (15)	0.02 (15)	-0.08 (15)	
390.9 (3)	25 (2)	-0.56 (4)	-0.02 (4)		
432.0 (2)	137 (7)	-0.42 (4)	-0.09 (4)	-0.06 (5)	
482.1 (5)	48 (4)				
525.7 (4)	13 (2)	-0.35 (20)	0.16 (20)		
800 (1) <sup>a</sup>					
823 (1) <sup>a</sup>	95 (20) <sup>a</sup>				
872.8 (3)	6 (2)	0.19 (25)	0.09 (25)		
922.3 (5)	36 (4)				
959.6 (3)	9 (3)				
1077.3 (6)	9 (3)				
1114.0 (6)	12 (3)				
1125 (1) <sup>a</sup>					

<sup>a</sup>From coincidence spectra.

<sup>b</sup> $P_{\text{cal}}$  was calculated assuming a pure stretched- $E2$  transition.

$$W(\theta) = a_0 + a_2 g_2 P_2(\cos\theta) + a_4 g_4 P_4(\cos\theta), \quad (1)$$

where  $W(\theta)$  is the normalized  $\gamma$ -ray intensity at angle  $\theta$  with respect to the beam direction, and the corrections for the solid angle subtended by the Ge(Li) detector were  $g_2 = 0.99$  and  $g_4 = 0.97$ . These angular distribution results are summarized in Table I.

### C. Linear polarizations

The experimentally measured asymmetry in the counting rate is defined as

$$\Delta = [N(90^\circ) - N(0^\circ)] / [N(90^\circ) + N(0^\circ)], \quad (2)$$

where  $N(0^\circ)$  and  $N(90^\circ)$  are the counting rates with the polarimeter axis oriented, respectively, parallel and perpendicular to the reaction plane. The polarization  $P$  can be related to  $\Delta$  by a positive efficiency  $Q$ , defined by  $Q = \Delta/P$ , which must be determined for the polarimeter and experimental conditions.

For mixed quadrupole/dipole transitions, the polarization can be given<sup>11,12</sup> in terms of the angular distribution coefficients  $A_2$  and  $A_4$ , as

$$P = \pm [3(A_2 + b_2) + 1.25A_4] / (2 - A_2 + 0.75A_4), \quad (3)$$

where

$$b_2 = \frac{-8A_2\delta F_2(12J_i J_f)}{3[F_2(11J_i J_f) + 2\delta F_2(12J_i J_f) + \delta^2 F_2(22J_i J_f)]}. \quad (4)$$

The sign in Eq. (3) is positive for  $E2/M1$  admix-

tures (no parity change) and is negative for  $M2/E1$  admixtures (parity change). The functions  $F(L_1 L_2 J_i J_f)$  are the standard correlation functions (see Ref. 13, for example), and  $\delta = \langle J_f | L_2 | J_i \rangle / \langle J_f | L_1 | J_i \rangle$  is the multipole mixing ratio defined for emission radiation in the phase convention of Biedenharn and Rose.<sup>14</sup>

The polarimeter calibration was effected using 29  $\gamma$  rays from  $^{64}\text{Zn}$ ,  $^{70}\text{Ge}$ ,  $^{78}\text{Kr}$ ,  $^{194}\text{Pt}$ , and  $^{196}\text{Pt}$  that ranged in energy from 250 to 2000 keV. These were all known stretched- $E2$   $\gamma$  rays whose polarizations could be calculated from their angular distribution coefficients using Eq. (3), and for which  $\Delta$  was measured experimentally. The efficiencies for these  $\gamma$  rays were fitted by least squares to the function

$$Q = Q_0(aE_\gamma + b), \quad (5)$$

where  $a$  and  $b$  are adjustable parameters and  $Q_0$  is the efficiency for the ideal case of two point detectors. This can be shown<sup>11,15</sup> from the Klein-Nishina formula to be

$$Q_0 = \frac{1 + (E_\gamma/m_0c^2)}{1 + (E_\gamma/m_0c^2) + (E_\gamma/m_0c^2)^2} \quad (6)$$

for a scattering angle of  $90^\circ$ , where  $m_0c^2$  is the electron mass in keV. The least-squares fit gave  $a = (-4 \pm 5) \times 10^{-5} \text{ keV}^{-1}$  and  $b = 0.62 \pm 0.03$ . Figure 1 in Ref. 10 shows a graph of  $Q$  as a function of  $E_\gamma$ , calculated with these parameters, and also the data points from which the least-squares fit

TABLE II. Summary of the coincidence relations of  $\gamma$  rays in  $^{76}\text{Br}$ . Weak coincidences are shown in parentheses. Known  $\gamma$  rays from other nuclides are identified.

Gate (keV)	Coincident $\gamma$ -ray transitions (keV)
73	73, 93, 112, 124, 142, 166, 199, (222), 238, (254), 331
93	73, (84), 112, 142, 238, (254), (350), (391), 432, (482), 823, (873), (922), (1114)
112	(73), 93, 142, 238, 331, (391), 432, 482, 800, 823
142	(73), 93, 112, (220), 222, 238, 331, (350), 432, (482), (800), 823, (898)
238	(73), 93, 112, 142, (210), 254, (355), (391), 432, (482), (526), (657), 800, 823, (1114)
254	73, 93, 104, 112, 124, 142, 166, 199, 222, 238, (254), 300, 331, 432, (482), 823
331	(73), 112, 142, 254, (300), (338), (355), (391), 432, (482), (651), (800), 823, (873), (922), (1114), (1125)
391	93, 112, 142, 199, 238, (254), 331, 424, <sup>b</sup> 432, (482)
432	93, 112, 142, 238, 254, 331, (350), 391, (427), (482), 873, 960, 1077, (1114), (1125)
482	93, 112, 142, (166), 199, (220), 238, (254), 300, 331, (375), 391, 432, 674, 823, (1114), (1125)
526	112, 142, 166, 199, 238
800 <sup>a</sup>	112, 142, 166, 199, 220, 238, (254), 295, 338, 424, <sup>b</sup> 559, <sup>c</sup> 618, <sup>b</sup> 736 <sup>b</sup>
823 <sup>a</sup>	93, 112, 142, 238, (254), 331, 424, <sup>b</sup> 482, 610, <sup>b</sup> (674), 1020, <sup>b</sup> (1114), (1125), (1188)
873	(93), (112), 142, 238, (254), 331, 350, 432
922 <sup>a</sup>	93, 112, 142, 238, (254), 331, 424, <sup>b</sup> 610, <sup>b</sup> 805 <sup>b</sup>
960	93, (112), 142, 238, 254, 331, 432, (526)
1077	(73), (93), 112, 142, 238, (254), 331, 432
1114	93, 112, 142, 238, (254), 331, (350), (391), (432), (482), 823, 1039
1125	112, 142, 238, (254), 331, (350), (391), 432, 482, 823, (1039)

<sup>a</sup>Doublet.

<sup>b</sup>From  $^{76}\text{Kr}$ .

<sup>c</sup>From  $^{76}\text{Se}$ .

was obtained.

The linear polarizations of the  $\gamma$  rays of  $^{76}\text{Br}$  are given in Table I. Also shown are polarizations, for transitions identified as stretched  $E2$ , calculated using Eq. (3) from the experimental  $A_2$  and  $A_4$  values with  $\delta = \infty$  and  $b_2 = 0$ .

#### D. Spin-parity assignments

The spin-parity assignments are given in Table III and are shown on the level scheme in Fig. 3. These have been assigned by using angular distributions and polarizations of  $\gamma$  rays as direct evidence. Further evidence was obtained from systematics of other nuclei in this mass region, and from the fact that in heavy-ion reactions,  $\gamma$ -ray cascades usually proceed from higher to lower spin. It was assumed that the observed transitions were of  $E1$ ,  $M1$ , or  $E2$  multipolarity, and consequently that if a spin change of  $\Delta J = 2$  were established between two levels and a  $\gamma$  ray transition were observed between them, then

they have the same parity.

The dependence of the theoretical angular distribution coefficients on the physical parameters is given (see Ref. 13, for example) by

$$A_k = \alpha_k(J_i) B_k(J_i) [F_k(11J_i J_f) + 2\delta F_k(12J_i J_f) + \delta^2 F_k(22J_i J_f)] / (1 + \delta^2), \quad (7)$$

where  $\alpha_k(J_i)$  are the attenuation coefficients of the alignment,  $B_k(J_i)$  are the statistical tensor elements for a system of nuclei completely aligned in a plane perpendicular to the beam direction,  $\delta$  is the multipole mixing ratio, and  $F(L_1 L_2 J_i J_f)$  are the standard correlation functions. It is assumed that the population of magnetic substates can be described by a Gaussian function involving only one parameter, so that  $\alpha_4(J_i)$  is uniquely related to  $\alpha_2(J_i)$ .

For possible values of the initial and final spins, the multipole mixing ratio  $\delta$  and the attenuation parameter  $\alpha_2(J_i)$  were varied in steps, and a

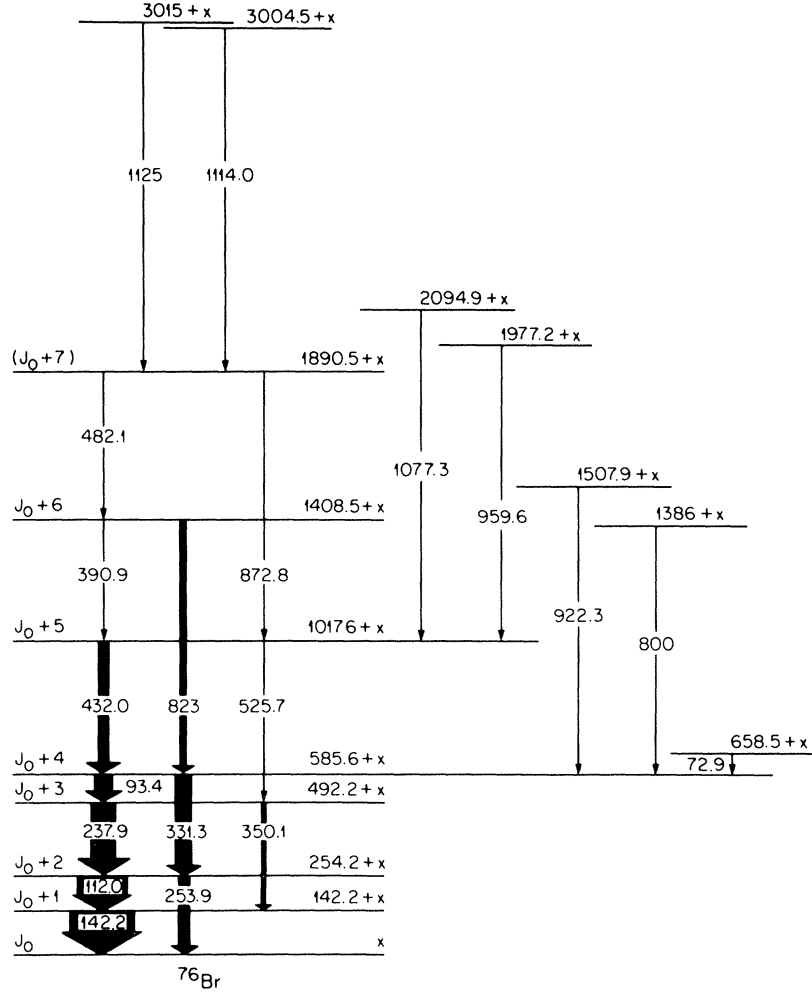


FIG. 3. Levels and transitions in  $^{76}\text{Br}$  observed with the  $^{66}\text{Zn}(^{12}\text{C}, p n \gamma)$  reaction. Energies are in keV. Level energies are least-squares adjusted to all of the  $\gamma$ -ray energies.

goodness-of-fit index  $\chi^2$  was calculated at each step, where

$$\begin{aligned} \chi^2 = & [A_{2 \text{ exp}} - A_{2 \text{ cal}}(J_i, J_f, \delta, \alpha_2)]^2 / \epsilon_{A_2}^2 \\ & + [A_{4 \text{ exp}} - A_{4 \text{ cal}}(J_i, J_f, \delta, \alpha_2)]^2 / \epsilon_{A_4}^2 \\ & + [P_{\text{exp}} - P_{\text{cal}}(J_i, J_f, \delta, \alpha_2)]^2 / \epsilon_P^2. \end{aligned} \quad (8)$$

$P_{\text{cal}}$  was calculated with Eqs. (3) and (4) using the  $A_{2 \text{ cal}}$  and  $A_{4 \text{ cal}}$  calculated with Eq. (7).  $\epsilon_{A_k}$  is the uncertainty in  $A_{k \text{ exp}}$ , and  $\epsilon_P$  is the uncertainty in  $P_{\text{exp}}$ . A value of  $\chi^2$  that corresponds to a probability of less than 1% in the event of a legitimate fit to the data was taken to exclude that combination of parameters.

The energy, spin, and parity of the bandhead were not established in this work. In discussing the properties of the other states in the band, we will specify the energy of the state above the

bandhead, and the spin and parity with respect to that of the bandhead, which we will designate  $J_0$  and  $\pi_0$ . In each case, the  $\chi^2$  calculations were carried out for both  $J_0 = 4$  and  $J_0 = 1$ , and the conclusions reached for spin and parity assignments were the same for both values of  $J_0$ .

*The 142-keV level.* The angular distribution of the 142-keV  $\gamma$  ray is compatible with spins of  $J_0 - 1$  and  $J_0 + 1$ . The polarization of this  $\gamma$  ray is compatible with both  $E2/M1$  and  $M2/E1$ , although somewhat favoring  $M2/E1$ . On the assumption that the cascade proceeds from higher to lower spin, we assign a spin of  $J_0 + 1$  to this level, in agreement with previous work.<sup>4</sup>

*The 254-keV level.* The angular distribution and polarization of the 254-keV  $\gamma$  ray are compatible with spins of  $J_0$  and  $J_0 + 2$ . The polarization of this  $\gamma$  ray is compatible with both  $E2/M1$  and  $M2/E1$ , although somewhat favoring  $M2/E1$ .

The angular distribution and polarization of the 254-keV  $\gamma$  ray are compatible with spins  $J_0 - 2$ ,  $J_0$ , and  $J_0 + 2$  with the same parity as the bandhead, and with spins  $J_0 - 1$ ,  $J_0$ , and  $J_0 + 1$  with opposite parity. We suggest that the spin is  $J_0 + 2$  with the same parity as the bandhead, in agreement with previous work.<sup>4</sup>

*The 492-keV level.* The angular distribution and polarization of the 238-keV  $\gamma$  ray are compatible with spins of  $J_0 + 1$  and  $J_0 + 3$  with the same parity as that of the 254-keV level, and with spin  $J_0 + 3$  with opposite parity. In the case of a change in parity, however, the transition would have predominantly  $M2$  character, which is considered improbable. The angular distribution of the 350-keV  $\gamma$  ray did not contribute additional information due to its large uncertainty. On the assumption that the cascade proceeds from higher to lower spin, we assign this level a spin of  $J_0 + 3$ , in agreement with previous work.<sup>4</sup> A  $\chi^2$  plot of the 238-keV  $\gamma$  ray for spin  $J_0 + 3$  and the two possible parities is shown in Fig. 4. The possibility of a change in parity is clearly ruled out, and this establishes the parity of the 492-keV level to be the same as that of the 254-keV level. Since the 254- and 350-keV  $\gamma$  rays, each for which  $\Delta J = 2$ ,

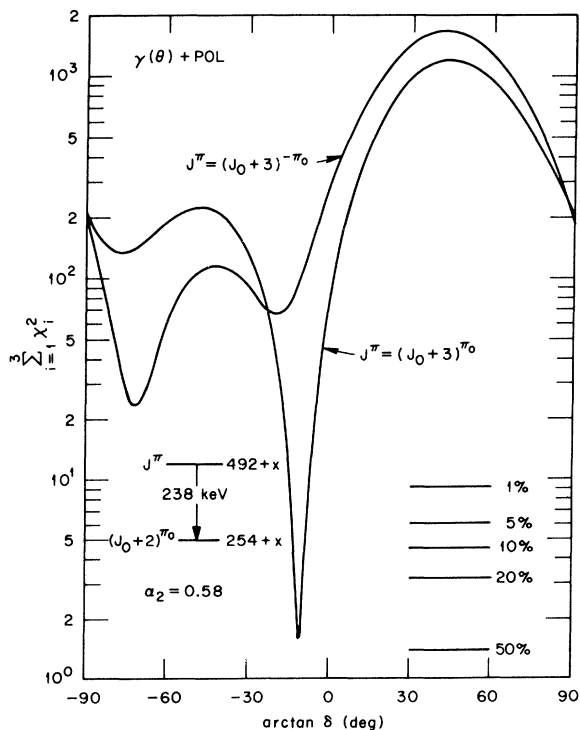


FIG. 4. Comparison between experimental and theoretical results for the angular distribution and polarization of the 238-keV  $\gamma$  ray as a function of  $\delta$  for  $\alpha_2 = 0.58$ . The calculation was made with  $J_0 = 4$ . The numbers in percent are the confidence limits.

are assumed to be stretched- $E2$  transitions, this establishes that the parities of the 492-, 254-, and 142-keV levels are all the same as that of the bandhead.

*The 586-keV level.* The angular distribution and polarization of the 331-keV  $\gamma$  ray are compatible with spins of  $J_0 + 2$  and  $J_0 + 4$  with the same parity as that of the 254-keV level, and with spins of  $J_0 + 1$  and  $J_0 + 3$  with opposite parity. The  $\chi^2$  fits strongly favor the cases with unchanged parity. The angular distribution of the 93-keV  $\gamma$  ray is compatible with spins of  $J_0 + 2$ ,  $J_0 + 3$ , and  $J_0 + 4$ . The polarization of this  $\gamma$  ray was not obtained. Assuming that the cascade proceeds from higher to lower spin, we assign this level a spin of  $J_0 + 4$  with the same parity as the bandhead in agreement with previous work.<sup>4</sup>

*The 1018-keV level.* The angular distribution and polarization of the 432-keV  $\gamma$  ray are compatible with  $J_0 + 3$  and  $J_0 + 5$  and favor the same parity as the 586-keV level. We suggest a spin of  $J_0 + 5$  with the same parity as the bandhead, in agreement with previous work.<sup>4</sup> The angular distribution of the 526-keV  $\gamma$  ray did not contribute additional information due to its large uncertainty. However, it is assumed to be a stretched- $E2$  transition, which supports the parity assignment.

*The 1409-keV level.* The angular distribution of the 391-keV  $\gamma$  ray is compatible with spins of  $J_0 + 4$  and  $J_0 + 6$ . Assuming that the cascade proceeds from higher to lower spin, we suggest a spin of  $J_0 + 6$  for this level. Assuming that the 823-keV  $\gamma$  ray is a stretched- $E2$  transition, we assign this level the same parity as the bandhead.

*The 1891-keV level.* The spin of this level is tentatively assigned  $J_0 + 7$  from systematics.

#### IV. DISCUSSION

In Table III we have summarized the level properties of  $^{76}\text{Br}$ . This table gives, for each level, the level energy above the bandhead, the spin and parity with respect to the bandhead, the  $\gamma$  rays depopulating the level and their branching ratios, and the multipole mixing ratio (deduced assuming  $J_0 = 4$ ) and multipolarity for each transition.

The levels and transitions of  $^{76}\text{Br}$  are shown in Fig. 3. We see a strongly excited  $\Delta J = 1$  band, plus a number of other levels that do not appear to be members of bands. We were not able to positively identify the bandhead. As pointed out by Lueders *et al.*,<sup>3</sup> the bandhead is probably not the ground state.

The spin and parity of the ground state have been assigned<sup>1,2</sup> the value  $1^-$ . On the basis of a Nilsson diagram appropriate for this region (we

TABLE III. Properties of the energy levels of  $^{76}\text{Br}$ .  $J_0$  and  $\pi_0$  are the spin and parity of the bandhead. The numbers in parentheses indicate probable errors in the last significant figures.

Level energy above bandhead (keV)	$J$	$\pi$	$E_\gamma$ (keV)	Branching ratio	$\delta^a$	Multipolarity
142.2 (2)	$J_0+1$	$\pi_0$	142.2	100	$-1.8 < \delta > -0.2$	$E2/M1$
254.2 (2)	$J_0+2$	$\pi_0$	253.9	14.6 (9)	$\varnothing$	$E2$
			112.0	85.4 (9)	$-2.4 < \delta > -0.3$	$E2/M1$
492.2 (2)	$J_0+3$	$\pi_0$	350.1	10.0 (23)	$\infty$	$E2$
			237.9	90.0 (23)	$-0.20$ (4)	$E2/M1$
585.6 (3)	$J_0+4$	$\pi_0$	331.3	49.7 (18)	$\infty$	$E2$
			93.4	50.3 (18)	$-0.08 < \delta > 0.02$	$E2/M1$
658.5 (3)			72.9	100	$\infty$	$E2$
1017.6 (3)	$J_0+5$	$\pi_0$	525.7	8.7 (13)	$\infty$	$E2$
			432.0	91.3 (13)	$-0.29$ (9)	$E2/M1$
1386 (1)			800	100		
1408.5 (4)	$J_0+6$	$\pi_0$	823	79 (4)	$\infty$	$E2$
			390.9	21 (4)	$-1.3 < \delta > -0.16$	$E2/M1$
1507.9 (6)			922.3	100		
1890.5 (4)	$(J_0+7)$	$(\pi_0)$	872.8	11 (3)	$(\infty)$	$(E2)$
			482.1	89 (3)		
1977.2 (4)			959.6	100		
2094.9 (4)			1077.3	100		
3004.5 (7)			1114.0	100		
3015 (1)			1125	100		

<sup>a</sup>Deduced assuming  $J_0=4$ .

choose the one given in Fig. 5 of Ref. 16, since it has been employed in a parameter-independent dynamic-deformation theory of different nuclei described in Ref. 17), the  $^{76}\text{Br}$  ground-state spin of  $1^-$  (as well as the ground-state spins of the neighboring odd- $p$  and odd- $n$  nuclei) can be understood in terms of a  $\frac{3}{2} [312]$  proton orbital coupled to a  $\frac{5}{2} [422]$  neutron orbital with deformation  $\beta \approx 0.35$ .

According to the rules of coupling the Nilsson orbitals (see, for example, the review article by Nathan and Nilsson<sup>18</sup>), such a coupling would lead to two almost degenerate intrinsic states: one with  $K = |\Omega_p - \Omega_n| = |\frac{3}{2} - \frac{5}{2}| = 1$  and one with  $K = \Omega_p + \Omega_n = 4$ . Since the parity of the proton orbital  $\frac{3}{2} [312]$  is negative and that of the neutron orbital  $\frac{5}{2} [422]$  is positive, the parity of the two coupled intrinsic states would be negative. Thus, in addition to a  $K^\pi = 1^-$  band with its bandhead forming the  $1^-$  ground state of  $^{76}\text{Br}$ , we would expect a  $K^\pi = 4^-$  band ( $J^\pi = 4^-, 5^-, 6^-, \dots$ ) whose bandhead ( $4^-$ ) may be identified with the bandhead of our observed band. However, this identification needs to be checked further by more detailed calculations, as well as experiments for the lifetimes, transition probabilities, and moments.

Schmidt-Ott *et al.*<sup>5</sup> and Kreiner *et al.*<sup>6</sup> have reported a long-lived isomer ( $T_{1/2} \approx 1.4$  s) in  $^{76}\text{Br}$  at 103 keV. This state decays to the  $2^-$  45.5-keV

state by a transition deduced to be of  $M2$  multiplicity by conversion-electron measurements, giving this isomer a spin and parity of  $4^+$ . A  $4^+$  state could be understood in terms of a  $\frac{3}{2} [431]$  proton orbital coupled to a  $\frac{5}{2} [422]$  neutron orbital with deformation  $\beta \approx 0.35$ . This  $4^+$  state at 103 keV could also possibly be the bandhead for our observed band. If either of these identifications is correct, then we have observed the band up to a spin of  $J=11$ .

In Fig. 5, we show a graph of the level energy

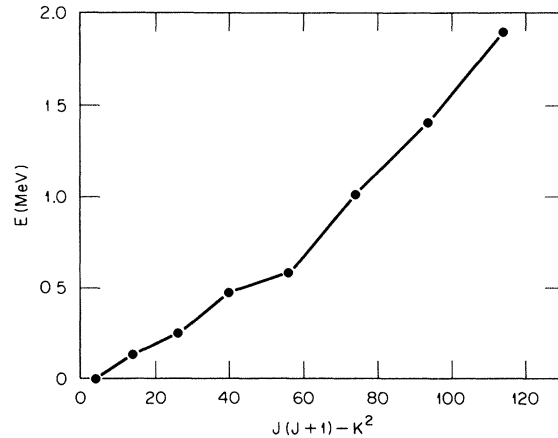


FIG. 5. Graph of the level energy above the bandhead versus  $J(J+1) - K^2$ , with  $J_0=4$  (see text) and  $K=4$ .

versus  $J(J+1) - K^2$ , where we have set  $J_0 = 4$  and  $K = 4$ . The slope of such a plot is the inverse of the moment of inertia,  $\hbar^2/2\theta$ . We see a definite change in the slope at the fourth level above the bandhead; for the lower levels, the slope has an average value of 12 keV, and for the higher levels, 22 keV. This abrupt break in the moment of inertia may indicate a band crossing at  $J = 8$ .

In Fig. 6, the quantity  $(E_J - E_{J-1})/2J$  is plotted as a function of  $J^2$ . In such a graph, a horizontal line would be expected if the moment of inertia were independent of the angular momentum, and a band following the equation  $E = AJ(J+1) + BJ^2$  ( $J+1$ )<sup>2</sup> would give a straight line with slope  $B$  (see, for example, Ref. 19). The zig-zag pattern up to spin  $J = 8$ , which is very obvious in this plot, and also to some extent in Fig. 5, can be attributed to a perturbation due to the Coriolis interaction, which produces a staggering effect by raising the excitation energies of alternate levels relative to the others (see, for example, the review article by Lieder and Ryde<sup>20</sup>). However, above this spin, the plot of  $(E_J - E_{J-1})/2J$  abruptly becomes more horizontal. This suggests the possibility of a band crossing at spin  $J = 8$ , with the lower-spin states being members of a rotation-aligned band with strong Coriolis decoupling of the odd proton and neutron, and the higher-spin states being members of a strong-coupled rotational band with less Coriolis decoupling.

There is an interesting similarity, shown in Fig. 7, in the spacings of the levels of <sup>76</sup>Br and <sup>74</sup>Br (from Ref. 21). This same pattern of level spacings in <sup>76</sup>Br, <sup>77</sup>Kr (from Ref. 22), and <sup>78</sup>Rb

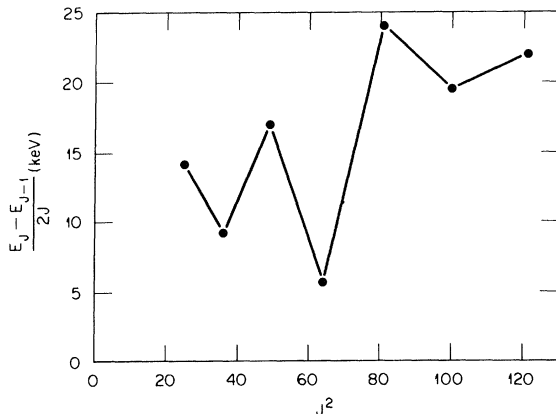


FIG. 6. Graph of the transition energy divided by twice the spin versus the square of the spin, with  $J_0 = 4$  (see text).

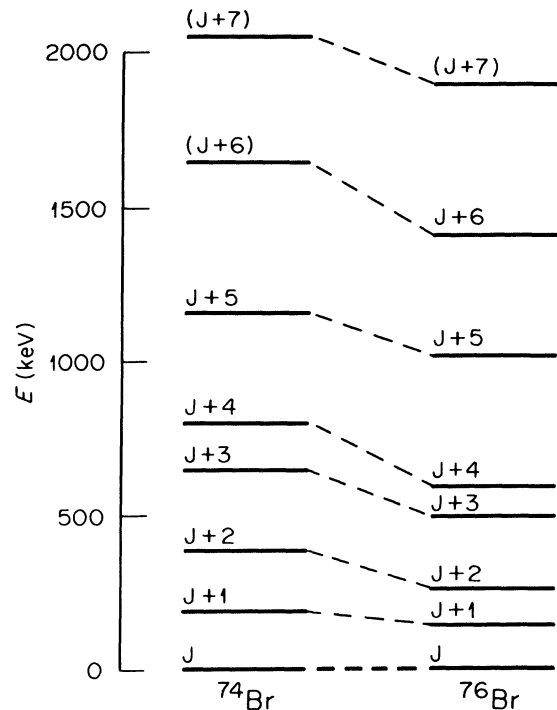


FIG. 7. Comparison of the energy levels of <sup>74</sup>Br and <sup>76</sup>Br.

(from Ref. 7) has been pointed out by Mariscotti *et al.*<sup>7</sup> and is shown in Fig. 8. Perhaps all of these bands can be described as rotation-aligned bands, and the similarities seen here indicate a relationship between the excitation mechanisms of the doubly odd and odd- $A$  nuclei.

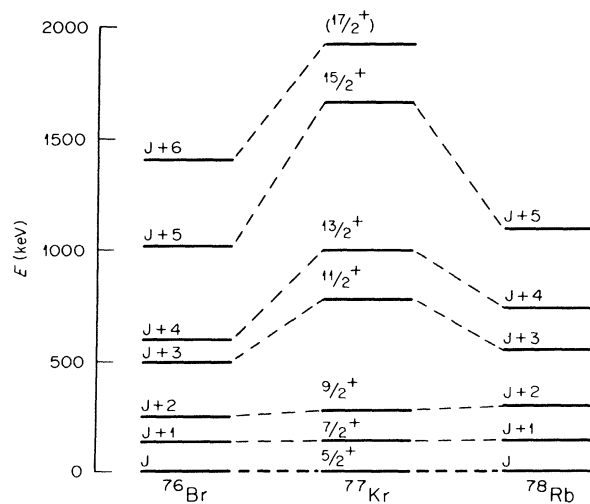


FIG. 8. Comparison of the energy levels of <sup>76</sup>Br, <sup>77</sup>Kr, and <sup>78</sup>Rb.



## ACKNOWLEDGMENTS

The research performed at the Oak Ridge National Laboratory was supported by the Division of Basic Energy Sciences, U. S. Department of

Energy, under Contract No. W-7405-eng-26 with Union Carbide Corporation. The research performed at Vanderbilt University was supported in part by a grant from the U. S. Department of Energy.

- 
- \*Present address: Physics Department, The Johns Hopkins University, Baltimore, Maryland 21218.  
 †Present address: Physics Department, Vanderbilt University, Nashville, Tennessee 37235.
- <sup>1</sup>T. Paradellis, A. Houdayer, S. K. Mark, Nucl. Phys. A201, 113 (1973).  
<sup>2</sup>D. Lode, W. Pessara, H. Ohlsson, and E. Roeckl, Z. Phys. 260, 253 (1973).  
<sup>3</sup>D. H. Lueders, J. M. Daley, F. E. Durham, S. G. Buccino, and C. E. Hollandsworth, Phys. Rev. C 17, 847 (1978).  
<sup>4</sup>M. Behar, A. Filevich, G. García Bermúdez, and M. A. J. Mariscotti, Nucl. Phys. A282, 331 (1977).  
<sup>5</sup>W. -D. Schmidt-Ott, A. J. Hautojärvi, and U. J. Schrewe, Z. Phys. A 289, 121 (1978).  
<sup>6</sup>A. J. Kreiner, G. García Bermúdez, M. A. J. Mariscotti, and P. Thieberger, Phys. Lett. 83B, 31 (1979).  
<sup>7</sup>M. A. J. Mariscotti, G. García Bermúdez, J. C. Acquadro, A. Lepine, M. N. Rao, W. Seale, E. der Mateosian, and P. Thieberger, Phys. Rev. C 19, 1301 (1979).  
<sup>8</sup>M. Behar, A. Filevich, G. García Bermúdez, M. A. J. Mariscotti, and L. Szybisz, Nucl. Phys. A337, 253 (1980).  
<sup>9</sup>K. A. Hardy, A. Lumpkin, Y. K. Lee, G. E. Owen, and R. Schnidman, Rev. Sci. Instrum. 42, 482 (1971).  
<sup>10</sup>J. C. Wells, Jr., R. L. Robinson, H. J. Kim, R. O. Sayer, A. J. Caffrey, and R. B. Piercey, Phys. Rev. C 18, 2162 (1978).  
<sup>11</sup>A. R. Poletti, E. K. Warburton, and J. W. Olness, Phys. Rev. 164, 1479 (1967).  
<sup>12</sup>L. W. Fagg and S. S. Hanna, Rev. Mod. Phys. 31, 711 (1959).  
<sup>13</sup>T. Yamazaki, Nucl. Data A3, 1 (1967).  
<sup>14</sup>L. C. Biedenharn and M. E. Rose, Rev. Mod. Phys. 25, 729 (1953).  
<sup>15</sup>H. Frauenfelder and R. M. Steffen, in *Alpha-, Beta-, and Gamma-Ray Spectroscopy*, edited by K. Siegbahn (North-Holland, Amsterdam, 1965), p. 1040 ff.  
<sup>16</sup>D. Ardouin, B. Remaud, K. Kumar, F. Guilbault, P. Avignon, R. Seltz, M. Vergnes, and G. Rotbard, Phys. Rev. C 18, 2739 (1978).  
<sup>17</sup>K. Kumar, in *Structure of Medium-Heavy Nuclei 1979*, Proceedings of a conference, Rhodes, Greece, 1979, edited by G. S. Anagnostatos, C. A. Kalfas, S. Kossionides, T. Paradellis, L. D. Skouras, and G. Vourvopoulos (Institute of Physics, Bristol, U. K., 1980), p. 169.  
<sup>18</sup>O. Nathan and S. G. Nilsson, in *Alpha-, Beta-, and Gamma-Ray Spectroscopy*, edited by K. Siegbahn (North-Holland, Amsterdam, 1965), p. 672.  
<sup>19</sup>F. S. Stephens, P. Kleinheinz, R. K. Sheline, and R. S. Simon, Nucl. Phys. A222, 235 (1974).  
<sup>20</sup>R. M. Lieder and H. Ryde, in *Advances in Nuclear Physics*, edited by M. Baranger and E. Vogt (Plenum, New York, 1978), Vol. 10, p. 57 ff.  
<sup>21</sup>R. B. Piercey, J. H. Hamilton, R. M. Ronningen, A. V. Ramayya, R. L. Robinson, and H. J. Kim, Program of the 43rd Meeting of the Southeastern Section of the American Physical Society, Old Dominion University, 1976 (unpublished), p. 4 and (private communication).  
<sup>22</sup>E. Nolte and P. Vogt, Z. Phys. A 275, 33 (1975).